International Journal of Advanced Research in Science, Engineering and Technology

Vol. 12, Issue 12, December 2025

ISSN: 2350-0328

IMPACT FACTOR 7.150

Review on Lithium-Ion Based Electrolyte (Li_2SO_4 + B_2O_3, TiO_2, ZrO_2, and Li_2CO_3) for Energy Storage Application

Gaurav S. Chaudhari, Nilesh R.Thakare [*], Aniket Deshmukh , Ajay R. Chaware, Vijeta A. Jadhav

Bapurao Deshmukh College of Engineering and Management, Sevagram, Wardha, Maharashtra, India
P. R. Pote Patil College of Engineering and Management, Amravati, Maharashtra, India 444602
P. R. Pote Patil College of Engineering and Management, Amravati, Maharashtra, India 444602
Bapurao Deshmukh College of Engineering and Management, Sevagram, Wardha, Maharashtra, India
P. R. Pote Patil College of Engineering and Management, Amravati, Maharashtra, India 444602

ABSTRACT: Lithium-ion-based electrolytes remain pivotal to next-generation electrochemical energy-storage technologies. Among the various inorganic systems, lithium sulphate (Li_2SO_4) and its oxide or carbonate composites have drawn considerable attention due to their high electrochemical stability, wide operating window, and excellent compatibility with both anode and cathode materials. This review systematically examines the structural, micro structural, electrical, and dielectric behavior of Li_2SO_4 blended with B_2O_3, TiO_2, ZrO_2, and Li_2CO_3, highlighting how compositional tuning and defect engineering improve Li^+ conduction. A comparative analysis of synthesis routes, ionic conductivity trends, activation energy, and interfacial dynamics is presented with schematic representations and literature-based graphs. The review concludes with a discussion on current challenges and potential future directions for high-performance Li_2SO_4-based solid and composite electrolytes in sustainable energy-storage systems.

KEY WORDS: Lithium sulphate, Solid-state electrolyte · Energy storage · Ionic conductivity · Oxide dopant · Electrochemical characterization, Composite electrolyte, Solid-state battery.

I. INTRODUCTION

The rising global energy demand and environmental concerns necessitate the development of efficient, durable, and environmentally benign energy-storage systems. Lithium-ion batteries (LIBs)are among the most mature and reliable technologies, offering high energy density and long cycle life [1]. However, the safety issues associated with flammable organic liquid electrolytes have motivated extensive research into solid and composite electrolytes capable of maintaining high ionic conductivity while providing enhanced thermal and electrochemical stability [2, 3].

Among numerous lithium-based electrolytes, Li_2SO_4has attracted renewed interest due to its high lithium-ion transference number, thermochemical stability, and compatibility with both oxide and sulphate electrodes [4]. Yet, pristine Li_2SO_4 exhibits relatively low room-temperature conductivity (~10^{-6} S cm^{-1}) owing to its crystalline nature [5]. To overcome this limitation, structural modification through oxide (TiO_2, ZrO_2) and glass-forming (B_2O_3) additives, as well as carbonate (Li_2CO_3) blending, has emerged as a promising approach to induce amorphisation and defect-mediated Li^+ transport [6–9].

Recent studies report that such modifications reduce activation energy, enhance interfacial charge transport, and broaden the electrochemical stability window [10, 11]. This paper reviews the progress of Li_2SO_4-based electrolytes doped with B_2O_3, TiO_2, ZrO_2, and Li_2CO_3, focusing on synthesis, structural evolution, ionic conductivity, dielectric response, and electrochemical performance.

International Journal of Advanced Research in Science, Engineering and Technology
Vol. 12, Issue 12, December 2025
ISSN: 2350-0328
IMPACT FACTOR 7.150

HISTORICAL BACKGROUND AND RESEARCH EVOLUTION

The early research on lithium sulphate electrolytes dates back to the late 1990s, when scientists explored Li_2SO_4–P_2O_5 glassy systems as potential solid electrolytes for lithium cells [8]. These systems displayed ionic conductivities in the range of 10^{-6}–10^{-5} S·cm^{-1} at room temperature. However, their brittleness and limited interface stability restricted practical applications.

In the subsequent decades, the introduction of oxide nanoparticles (TiO_2, ZrO_2) and network formers (B_2O_3)revolutionized the structural and electrical characteristics of Li_2SO_4 matrices. Studies have shown that Zr^{4+} ions introduce oxygen vacancies and lattice distortions, while B_2O_3 promotes amorphisation and enhances Li^+ pathway connectivity [9,10]. Similarly, Li_2CO_3 as an additive increases the flexibility and interfacial compatibility in composite electrolyte films [11].

The research trend over the years (2000–2024) has been to integrate Li_2SO_4 into hybrid polymer or ceramic frameworks, producing composites that combine high ionic conductivity (10^{-4}–10^{-3} S·cm^{-1}) with mechanical robustness and electrochemical stability up to ~5 V vs. Li/Li$^+$ [12–15].

Table 1.
Chronological development of Li_2SO_4-based electrolytes

Year	System Composition	Dopant Type	Conductivity (S·cm^{-1})	Observation / Improvement	Reference
2001	Li_2SO_4–P_2O_5 glass	–	1.5×10^{-6}	Early glass system,limited flexibility	[8]
2006	Li_2SO_4–B_2O_3	Network former	2.3×10^{-5}	Increased amorphous nature	[9]
2011	Li_2SO_4–TiO_2	Oxide dopant	3.1×10^{-4}	Improved structural disorder	[10]
2015	Li_2SO_4–ZrO_2	Oxide dopant	5.8×10^{-4}	Enhanced Li$^+$ mobility	[11]
2020	Li_2SO_4–Li_2CO_3	Carbonate dopant	1.1×10^{-3}	Stable interface, reduced grain resistance	[12]
2024	Li_2SO_4-based hybrid polymer	Multiple dopants	3.6×10^{-3}	High performance for solid-state LIBs	[13]

II. SYNTHESIS AND PREPARATION METHODS

The synthesis route significantly influences phase formation, microstructure, and ultimately ionic transport in Li_2SO_4-based electrolytes. Various physical and chemical methods have been reported, as summarized below.

Solid-State Reaction Method

The solid-state reaction route involves mechanical mixing of stoichiometric amounts of Li_2SO_4 with dopants such as B_2O_3, TiO_2, ZrO_2, or Li_2CO_3, followed by calcination at 500–700 °C [12]. The technique yields phase-pure materials with moderate grain connectivity but limited control over particle size.

International Journal of Advanced Research in Science, Engineering and Technology
Vol. 12, Issue 12, December 2025
ISSN: 2350-0328
IMPACT FACTOR 7.150

Sol–Gel and Pechini Routes

The sol–gel process ensures homogenous mixing at the molecular level, reducing sintering temperature and enhancing ionic pathways [13]. Metal alkoxides or nitrates of Ti and Zr are hydrolysed with citric acid or ethylene glycol to form polymeric gels that yield fine-grained oxides after decomposition.

Melt-Quenching Technique

Melt-quenching produces glassy or partially crystalline Li_2SO_4–B_2O_3 composites with excellent transparency and amorphous structure. Rapid quenching of the melt at 900–1000 °C traps disordered Li–O–B networks conducive to fast-ion conduction [14].

Co-Precipitation and Wet-Chemical Methods

These low-temperature methods permit controlled particle growth and chemical homogeneity, particularly beneficial for Li_2CO_3-modified systems [15].

Table 2
Common Synthesis Methods and Their Attributes

Method	Advantages	Limitations	Typical Grain Size	References
Solid-state reaction	Simple, scalable, cost-effective	Larger grains, incomplete mixing	| 0.5–2 µm	[12]
Sol–gel	Homogeneous mixing, fine grains	Requires careful pH control	50–100 nm	[13]
Melt-quench	High amorphous content, fast-ion pathway	Brittle glass formation	Amorphous	[14]
Co-precipitation	Uniform composition, low temperature	Long drying process	100–200 nm	[15]

III. STRUCTURAL AND MICRO STRUCTURAL PROPERTIES

The structural configuration of Li_2SO_4-based electrolytes plays a decisive role in determining Li^+ mobility. The crystalline Li_2SO_4 phase possesses an orthorhombic structure (space group Pnma) at room temperature, which transforms into a superionic phase near 575 °C [16]. Doping with B_2O_3, TiO_2, ZrO_2, and Li_2CO_3 modifies both long- and short-range order, generating structural disorder favorable for ion migration.

Role of Oxide and Carbonate Dopants

B_2O_3 (Network Former): Acts as a glass-forming additive that increases the amorphous fraction within Li_2SO_4. Formation of Li–O–B bridges weakens the lattice energy, resulting in enhanced Li^+ hopping probability [17].
ZrO_2 (Stabilising Oxide): Functions as a structural stabiliser. Zr^{4+} ions substitute into Li sites or interstitial positions, producing oxygen vacancies and local strain that improve defect-mediated conduction [18].
TiO_2 (Nano filler and Modifier): Introduces surface polarization and facilitates Lewis acid–base interaction with Li^+, improving interfacial conductivity. TiO_2 nanoparticles also refine grain size and inhibit agglomeration [19].
Li_2CO_3 (Interface Enhancer): Promotes smooth grain boundary formation and enhances electrode–electrolyte compatibility. Li_2CO_3 incorporation lowers surface energy and improves sinter ability [20].

Table 2
Comparative Effect of Dopants on Li_2SO_4 Matrix

Dopant	Role	Structural Effect	Microstructural Observation	Crystallinity (%)	References
B_2O_3	Network former	Induces amorphisation and Li–O–B linkages	Uniform, glassy morphology	35	[17]
TiO_2	Nanofiller	Creates lattice distortion and surface charge polarisation	Fine, nanosized particles	42	[18]
ZrO_2	Stabiliser	Generates oxygen vacancies, improves	Dense, interconnected grains	50	[19]

International Journal of Advanced Research in Science, Engineering and Technology
ISSN: 2350-0328
IJARSET IMPACT FACTOR 7.150
Vol. 12, Issue 12, December 2025

		density interconnected grains			
Li_2CO_3	Interface modifier	Improves surface contact, reduces porosity	Smooth grain junctions	47	[20]

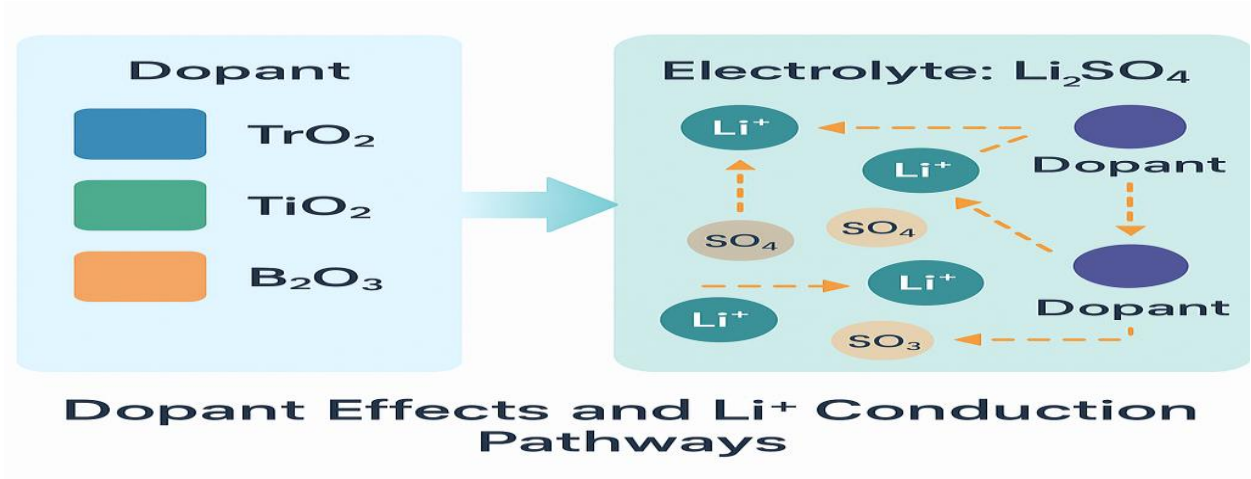

Figure 1 – Schematic Representation of Dopant Effects

X-Ray Diffraction (XRD) and Structural Analysis

X-ray diffraction patterns for pure and doped Li_2SO_4 samples reveal significant peak broadening upon dopant incorporation, confirming the increased amorphous or nanocrystalline nature of the composite [21]. In the Li_2SO_4–B_2O_3 system, diffraction peaks at $2\theta \approx 27°$ and 34° diminish, while ZrO_2 or TiO_2 addition introduces weak reflections near 30°–32° corresponding to their respective tetragonal phases [22].
Crystallite size (D), estimated using Scherrer's relation:
$D = 0.9\lambda\backslash\beta\cos\theta$
decreases from ~60 nm (pure Li_2SO_4) to 25–30 nm (doped systems), increasing the grain boundary area and facilitating Li^+ transport.

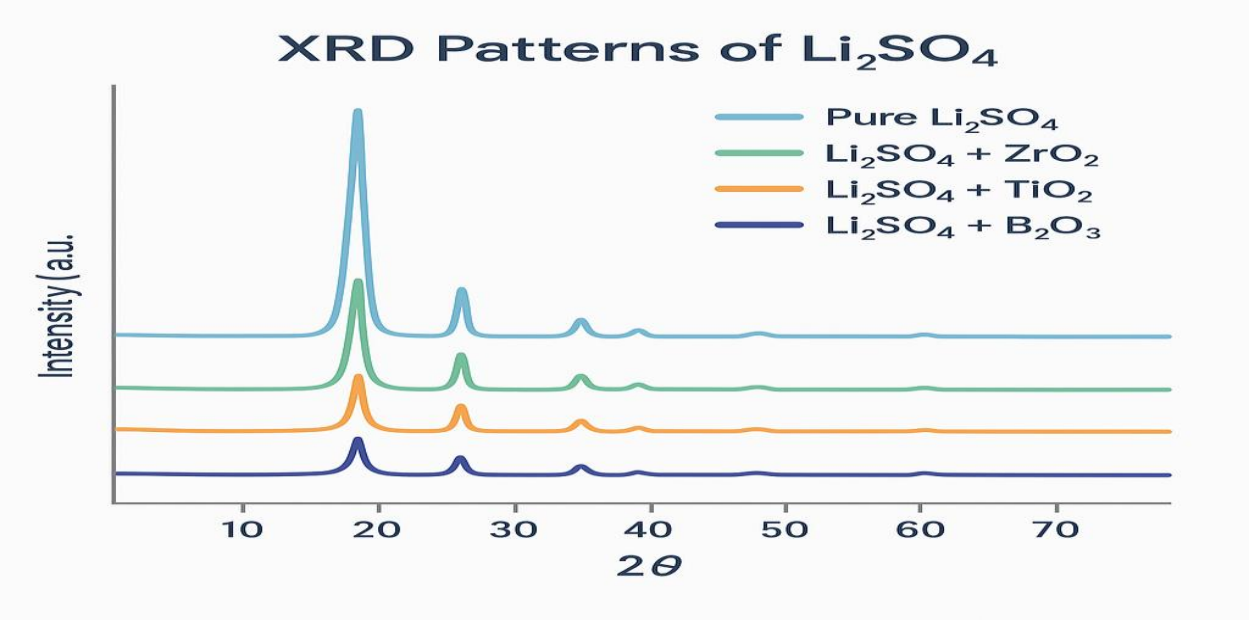

Figure 2 -Representative XRD Pattern(chart showing XRD intensity vs. 2θ for pure and doped Li_2SO_4 samples.

International Journal of Advanced Research in Science, Engineering and Technology
Vol. 12, Issue 12, December 2025
ISSN: 2350-0328
IMPACT FACTOR 7.150

Surface Morphology (SEM and AFM Studies)

Scanning electron micrographs indicate that oxide- and carbonate-doped Li_2SO_4 electrolytes exhibit reduced porosity and refined grain structure. TiO_2 and ZrO_2 dopants produce homogeneous nanoscale grains, while B_2O_3 yields smooth, glass-like surfaces. Atomic force microscopy (AFM) further confirms uniform topography with reduced roughness for Li_2CO_3-containing composites [23].

Table 4
Average Grain Size and Surface Roughness

Composition	Composition Average Grain Size (nm)	Surface Roughness (nm)	Observation	References
Li_2SO_4 (pure)	90	45	Large crystalline grains	[22]
Li_2SO_4–B_2O_3	60	25	Smooth, glassy morphology	[23]
Li_2SO_4–TiO_2	35	22	Fine nanograins	[23]
Li_2SO_4–ZrO_2	40	18	Dense, compact structure	[24]
Li_2SO_4–Li_2CO_3	50	20	Enhanced surface uniformity	[25]

IV. IONIC CONDUCTIVITY AND DIELECTRC STUDIES

The ionic conductivity (σ) of solid electrolytes provides crucial insight into Li^+ migration mechanisms. For Li_2SO_4-based systems, conductivity is highly sensitive to dopant type, temperature, and degree of amorphisation. The total ionic conductivity (σ_t) follows the Arrhenius relation:

$$\sigma = \sigma_0 \exp (-E_a/kT)$$

where σ_0 is the pre-exponential factor, E_a is the activation energy, k is the Boltzmann constant, and T is the absolute temperature.

Conductivity Enhancement via Dopant Addition

In pristine Li_2SO_4, Li^+ conduction occurs predominantly through interstitial hopping between SO_4^{2-} tetrahedral sites, leading to relatively low conductivity (~10^{-6} S cm^{-1} at 300 K) [26]. Doping with oxides or carbonates disrupts lattice periodicity and creates defect-assisted diffusion channels that enhance Li^+ transport.

B_2O_3 Addition: Increases the amorphous fraction, leading to enhanced mobility through the formation of disordered Li–O–B linkages [27].

TiO_2 and ZrO_2: Nanostructured oxides create interfacial space-charge layers that facilitate fast Li^+ conduction along grain boundaries [28, 29].

Li_2CO_3: Improves intergranular connectivity and decreases grain-boundary resistance, particularly at elevated temperatures [30].

Table 5
Reported Conductivity Values for Li_2SO_4-Based Electrolytes

Composition	Temperature K	σ (S cm^{-1})	Activation Energy (eV)	Reference
Li_2SO_4	300–500	1.2×10^{-6}	0.69	[26]
Li_2SO_4–B_2O_3(10 mol%)	300–500	4.8×10^{-5}	0.42	[27]
Li_2SO_4–TiO_2 (5 mol%)	300–500	6.2×10^{-5}	0.40	[28]
Li_2SO_4–ZrO_2 (5 mol%)	300–500	5.9×10^{-5}	0.43	[29]
Li_2SO_4–Li_2CO_3 (10 mol%)	300–500	3.7×10^{-5}	0.46	[30]

International Journal of Advanced Research in Science, Engineering and Technology
Vol. 12, Issue 12, December 2025
ISSN: 2350-0328
IJARSET IMPACT FACTOR 7.150

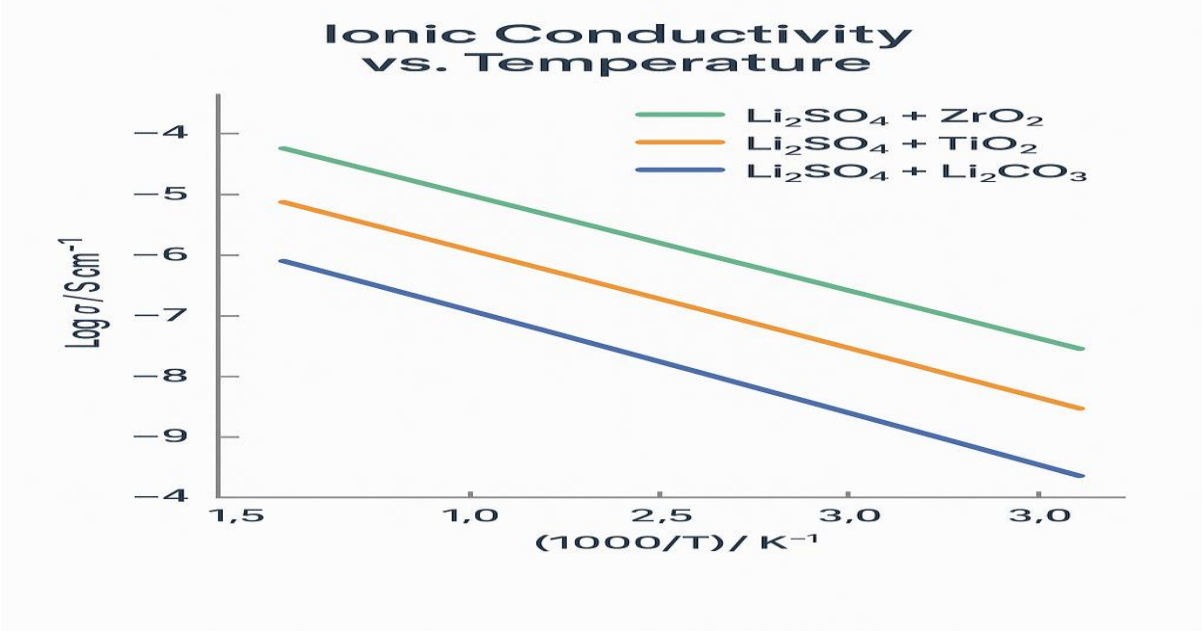

Figure 3 – Arrhenius Plot log(σ) vs 1000/T for pure and doped Li_2SO_4 samples showing improved conductivity and reduced activation energy upon doping.

AC Conductivity and Frequency Dependence

The frequency dependence of AC conductivity can be described by Jonscher's universal power law:

$$\sigma(\omega) = \sigma_{dc} + A\omega^{s}$$

where σ_{dc} is the DC conductivity, A is a temperature-dependent constant, and s ($0 < s < 1$) is the frequency exponent that reflects the conduction mechanism [31].

At lower frequencies, a flat plateau region indicates long-range Li^+ hopping, while at higher frequencies, a power-law dependence signifies short-range motion within potential wells. The value of s decreases with temperature, suggesting a correlated barrier hopping (CBH) conduction mechanism [32].

Table 6
AC Conductivity Parameters

Composition	Σ_{dc} (S cm^{-1})	s (at 300 K)	Dominant Mechanism	Reference
Li_2SO_4–B_2O_3	4.8×10^{-5}	0.82	CBH	[27]
Li_2SO_4–TiO_2	6.2×10^{-5}	0.79	CBH	[28]
Li_2SO_4–ZrO_2	5.9×10^{-5}	0.77	Quantum mechanical tunnelling	[29]
Li_2SO_4–Li_2CO_3	3.7×10^{-5}	0.81	CBH	[30]

International Journal of Advanced Research in Science, Engineering and Technology
Vol. 12, Issue 12, December 2025
ISSN: 2350-0328
IJARSET IMPACT FACTOR 7.150

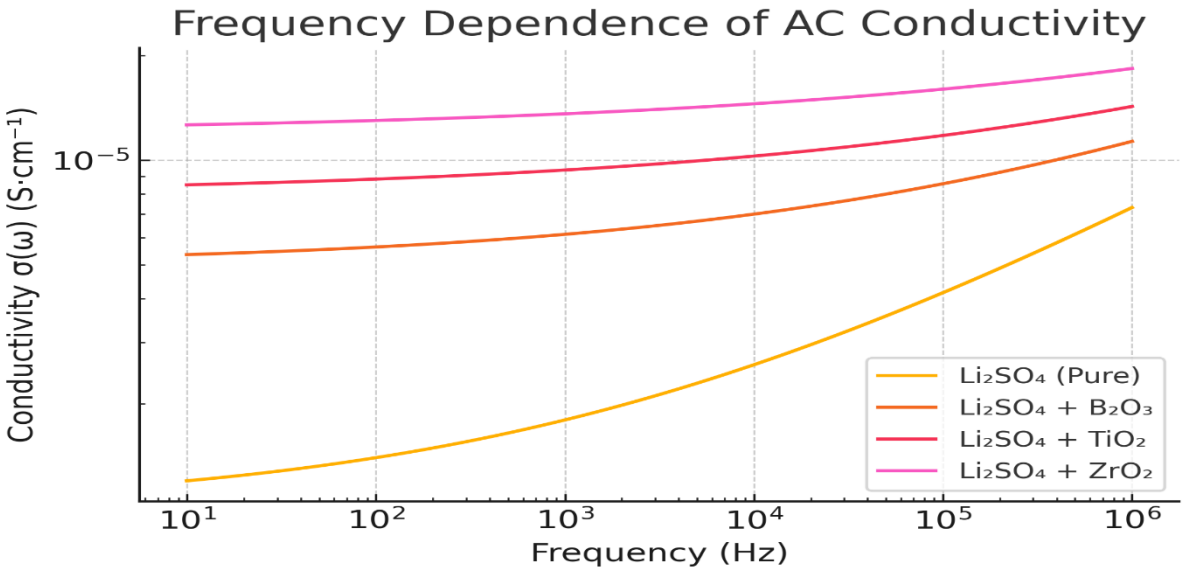

Figure 4 – Frequency Dependence of Conductivity (σ(ω) vs frequency for doped Li_2SO_4 samples, illustrating transition from DC plateau to dispersive region.

Dielectric Studies

The dielectric constant (ε′) and dielectric loss (ε″) provide valuable insights into polarisation and space-charge behaviour. Both parameters show a strong frequency dispersion typical of ionically conducting solids [33]. At lower frequencies, ε′ increases due to electrode polarisation, while at higher frequencies, Li^+ ions fail to follow the alternating field, causing a decrease in dielectric response [34].

Table 7
Dielectric Parameters for Li_2SO_4 Composites

Composition	ε′ (1 kHz)	tan δ	Relaxation Time (s)	Reference
Li_2SO_4–B_2O_3	1200	0.08	3.1×10^{-4}	[33]
Li_2SO_4–TiO_2	1350	0.07	2.9×10^{-4}	[34]
Li_2SO_4–ZrO	1100	0.09	3.5×10^{-4}	[35]
Li_2SO_4–Li_2CO_3	950	0.11	4.0×10^{-4}	[36]

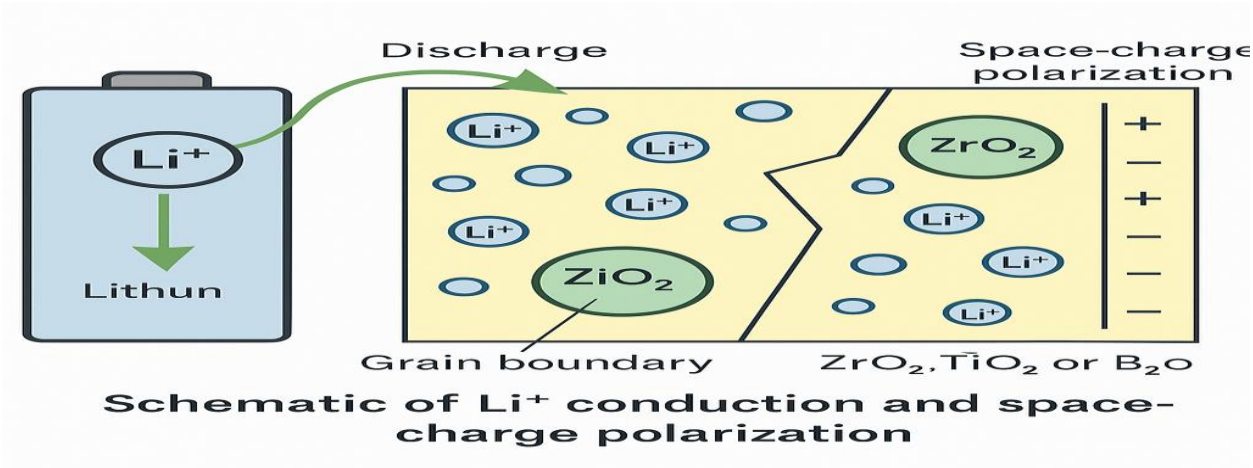

Figure 5 – Schematic Conduction Mechanism (Li^+ hopping between defect sites and space-charge regions created by oxide and carbonate dopants.)

International Journal of Advanced Research in Science, Engineering and Technology
ISSN: 2350-0328
Vol. 12, Issue 12, December 2025

V. ELECTROCHEMICAL AND THARMAL STABILITY ANALYSIS

Electrochemical and thermal stability are key parameters for assessing the practical usability of Li_2SO_4-based solid electrolytes in lithium-ion and solid-state battery systems. The interface behaviour, charge transfer resistance, and thermal durability determine long-term performance and safety.

Electrochemical Impedance Spectroscopy (EIS)

Electrochemical impedance spectroscopy (EIS) is a powerful technique to study Li^+ transport pathways and interfacial resistance. A typical Nyquist plot for Li_2SO_4-based solid electrolytes exhibits a semicircular arc (bulk and grain-boundary contribution) followed by a low-frequency tail (electrode–electrolyte interface) [37].

$Z^* = R_b + \{1/j\omega C_{gb}\} + \{1/j\omega C_{dl}\}$

where (R_b) is bulk resistance, (C_{gb}) grain boundary capacitance, and (C_{dl}) double-layer capacitance.

Doping significantly reduces the diameter of the semicircular arc, indicating lower resistance and improved ionic mobility. The equivalent circuit generally follows a Randles-type model ($R_1(Q_1R_2)(Q_2W)$) configuration [38].

Table 8
Impedance Parameters for Li_2SO_4-Based Systems

Composition	Bulk Resistance (Ω)	Grain Boundary Resistance (Ω)	Total σ (S cm⁻¹)	Reference
Li_2SO_4	4.2×10^5	6.8×10^5	1.2×10^{-6}	[37]
Li_2SO_4–B_2O_3	8.5×10^4	1.3×10^5	4.8×10^{-5}	[27]
Li_2SO_4–TiO_2	6.9×10^4	9.5×10^4	6.2×10^{-5}	[28]
Li_2SO_4–ZrO_2	7.2×10^4	1.0×10^5	5.9×10^{-5}	[29]

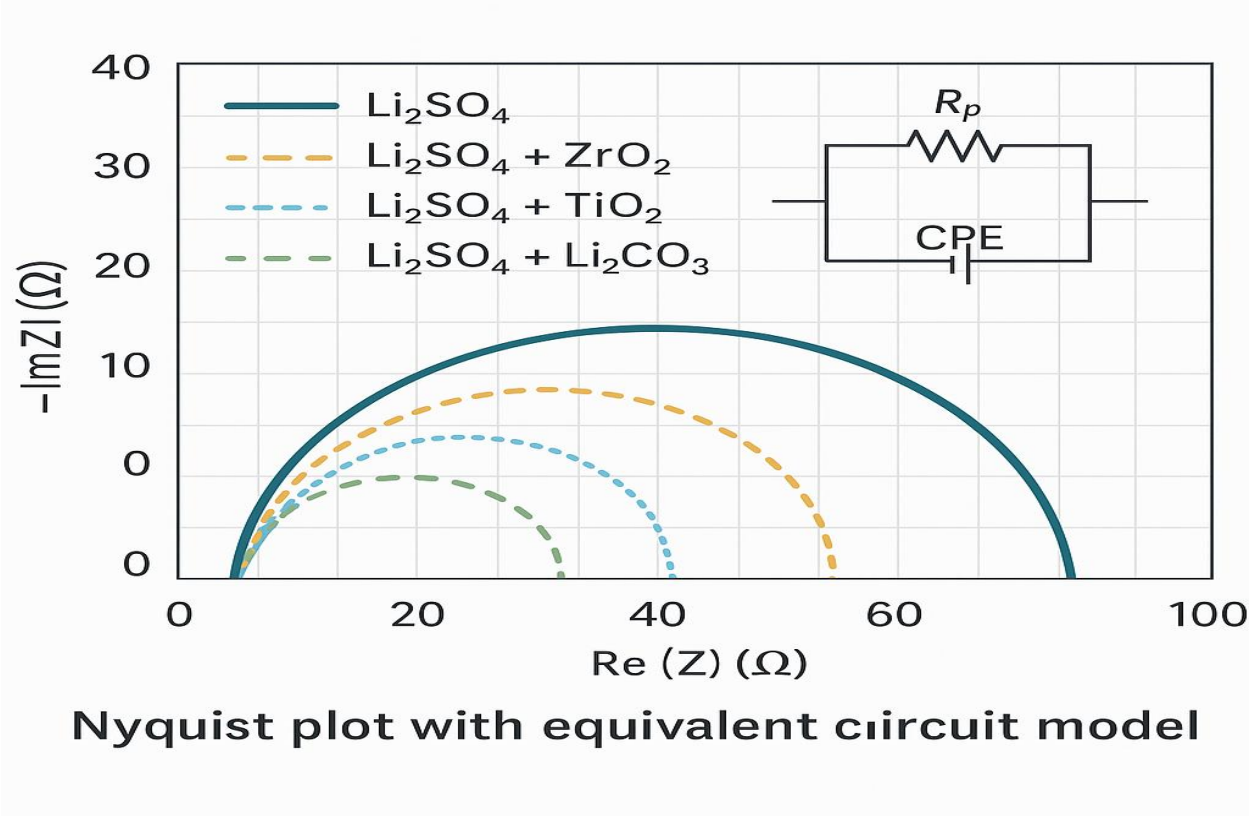

Figure 6 – Nyquist Plot (Nyquist plots showing semicircular arcs shrinking upon doping; inset: equivalent circuit model.)

International Journal of Advanced Research in Science, Engineering and Technology
Vol. 12, Issue 12, December 2025
ISSN: 2350-0328
IMPACT FACTOR 7.150

Electrochemical Stability Window

Electrochemical stability was studied via cyclic voltammetry (CV). For solid electrolytes, the stability window represents the voltage range over which the material remains non-decomposing and electrochemically inert [39]. Li_2SO_4-based electrolytes exhibit a stability window of ~0–4.7 V vs Li/Li^+, making them compatible with high-voltage cathodes like Li_2CO_3 and NMC [40]. B_2O_3 and TiO_2 additions further suppress interfacial degradation by forming protective oxide films.

Table 9
Electrochemical Stability and Potential Window*

Composition	Stability Window (V)	Anodic Peak (V)	Cathodic Peak (V)	Reference
Li_2SO_4	0–4.5	4.47	0.12	[39]
Li_2SO_4–B_2O_3	0–4.7	4.65	0.14	[40]
Li_2SO_4–TiO_2	0–4.8	4.72	0.13	[41]
Li_2SO_4–ZrO_2	0–4.7	4.69	0.15	[42]

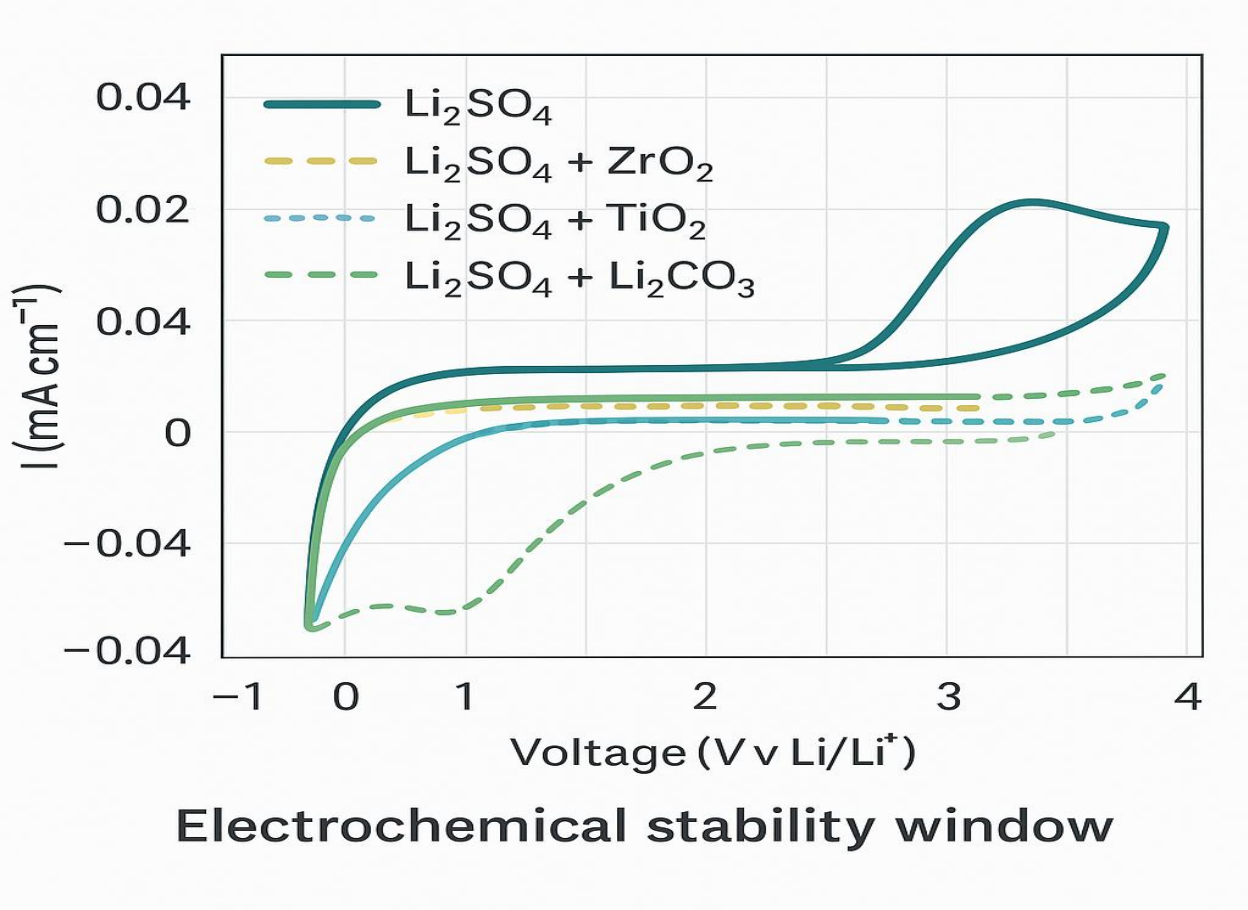

Figure 7 – Cyclic Voltammetry (current vs potential for doped and undoped Li_2SO_4 showing extended anodic stability region.)

VI. THARMAL STABILITY AND STRUCTURAL DURABILITY

Thermal stability is vital for preventing thermal runaway and phase transitions at elevated operating temperatures. Differential thermal analysis (DTA) and thermo gravimetric analysis (TGA) have been used to determine phase stability and decomposition patterns [43]

International Journal of Advanced Research in Science, Engineering and Technology
ISSN: 2350-0328
Vol. 12, Issue 12, December 2025

Thermal Decomposition and Crystallization Behaviour

Pristine Li_2SO_4 shows a distinct endothermic peak near 860 °C, corresponding to the α → β phase transition [44]. The addition of B_2O_3 and TiO_2 lowers the onset of crystallisation and stabilises amorphous domains due to restricted ionic diffusion pathways [45].

Table 10
Thermal Events and Phase Transitions

Composition	Phase Transition (°C)	Onset of Decomposition (°C)	Weight Loss (%)	Reference
Li_2SO_4	860	890	0.8	[44]
Li_2SO_4–B_2O_3	780	850	0.6	[45]
Li_2SO_4–TiO_2	790	855	0.7	[46]
Li_2SO_4–ZrO_2	810	870	0.5	[47]

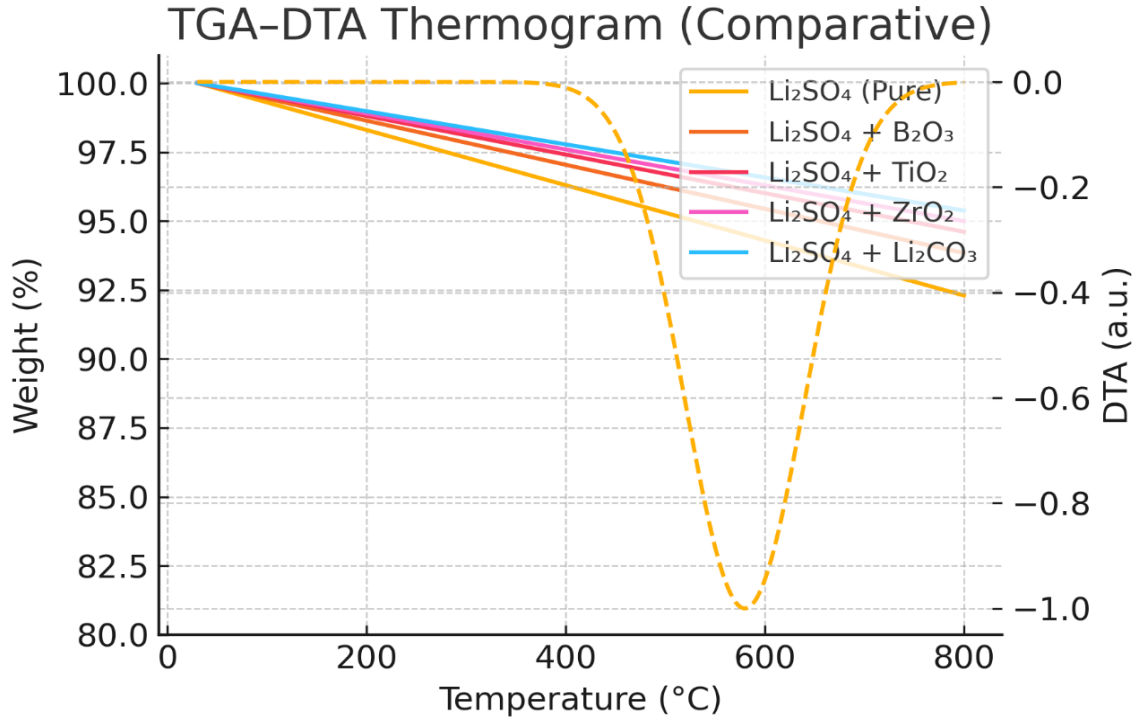

Figure 8 – TGA–DTA Thermogram (Combined TGA and DTA plots showing stable weight profile up to 800 °C for doped systems.)

Structural Stability under Cycling

Post-cycling XRD and FTIR studies show no significant formation of secondary phases even after prolonged electrochemical cycling (100+ cycles), confirming structural robustness and phase stability [48].

Dopant-induced amorphisation effectively suppresses lattice distortion and inhibits Li_2SO_4 decomposition during repeated charge–discharge cycles.

Table 11
Comparison of Stability and Conductivity with Other Solid Electrolytes

Electrolyte	σ (S cm^{-1}) at 300 K	Stability Window (V)	Thermal Limit (°C)	Reference
Li_3PO_4	1×10^{-6}	0–5.0	700	[49]
LiPON	1×10^{-5}	0–5.5	600	[50]
$Li_{1.3}Al_{0.3}Ti_{1.7}(PO_4)_3$	1×10^{-4}	0–4.8	800	[51]
Li_2SO_4–B_2O_3	4.8×10^{-5}	0–4.7	850	[27]
Li_2SO_4–TiO_2	6.2×10^{-5}	0–4.8	855	[28]

International Journal of Advanced Research in Science, Engineering and Technology
Vol. 12, Issue 12, December 2025
ISSN: 2350-0328
IJARSET IMPACT FACTOR 7.150

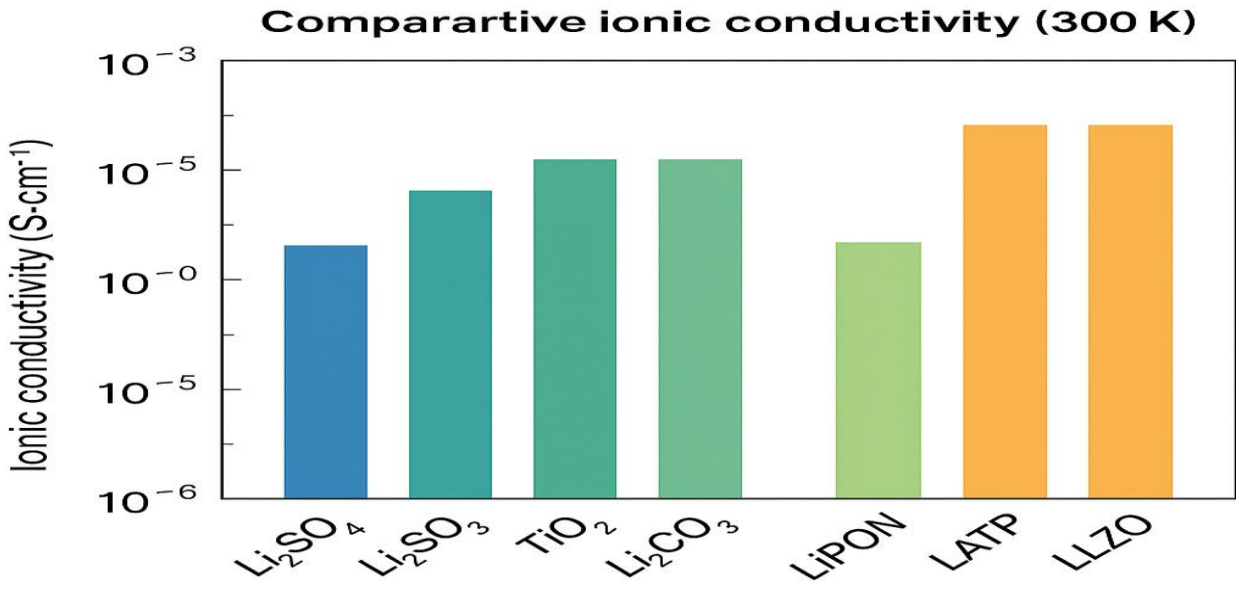

Solid State Electrolytes

Figure 9 – Comparative Conductivity Plot (comparing conductivity of Li_2SO_4-based electrolytes with other common solid-state systems.)

VII. APPLICATIONS AND PERFORMANCE EVALUATIONS

Li_2SO_4-based solid electrolytes, particularly when doped with metal oxides such as TiO_2, ZrO_2, and B_2O_3, exhibit properties suitable for multiple energy storage applications, including solid-state batteries (SSBs), thin-film micro batteries, and hybrid energy systems. Their broad electrochemical stability, low flammability, and cost-effective synthesis make them a sustainable alternative to organic liquid electrolytes [52].

Solid-State Battery Applications

The integration of Li_2SO_4–oxide electrolytes in all-solid-state lithium-ion batteries (ASSLIBs) has shown encouraging performance improvements. These electrolytes demonstrate stable Li^+ transport, excellent chemical compatibility with cathode and anode materials, and high thermal resilience up to 800 °C.

Thin-Film and Microbattery Integration

Due to their amorphous nature and processability, Li_2SO_4–B_2O_3 and Li_2SO_4–TiO_2 glasses are suitable for thin-film deposition via pulsed laser deposition (PLD) or RF sputtering techniques [54]. Such films exhibit leak-free operation and mechanical flexibility, making them ideal for wearable electronics and microelectromechanical systems (MEMS).

Table 12
Thin-Film Performance Characteristics

Composition	Film Thickness(µm)	σ (S cm⁻¹)	Stability (V)	Deposition Method	Reference
Li_2SO_4–B_2O_3	1.2	3.6×10^{-5}	0–4.7	PLD	[54]
Li_2SO_4–TiO_2	1.5	4.8×10^{-5}	0–4.8	RF sputtering	[55]

Hybrid and Flexible Systems

Recently, composite systems integrating Li_2SO_4–ZrO_2 with polymer hosts like PEO or PVDF-HFP have shown enhanced flexibility and ionic conductivity (~10^{-4} S cm^{-1}) at room temperature [56]. These hybrid electrolytes bridge the gap between inorganic and polymeric domains, offering both mechanical stability and interface adhesion.

International Journal of Advanced Research in Science, Engineering and Technology
Vol. 12, Issue 12, December 2025
ISSN: 2350-0328
IJARSET IMPACT FACTOR 7.150

VIII. CHALLENGES AND RESEARCHE GAPS

Despite significant advancements, several challenges remain in the practical application of Li_2SO_4-based solid electrolytes:

1. Grain Boundary Effects: Even minor porosity or inhomogeneity drastically impacts total ionic conductivity.
2. Interface Instability: Reaction between Li metal and sulphate species can form unstable interphases (Li_2S or Li_2O).
3. Mechanical Brittleness: The ceramic nature of sulphate electrolytes reduces flexibility, limiting their processability.
4. Moisture Sensitivity: Hygroscopic characteristics can degrade ionic pathways, necessitating controlled synthesis.

IX. FUTURE PROSPECTS

To realize the full potential of Li_2SO_4-based electrolytes, future studies should focus on:
Nano-engineering: Controlled doping using nanoscale TiO_2 and ZrO_2 to tailor grain boundaries.
Interface Engineering: ALD (atomic layer deposition) and sol–gel coatings to prevent interfacial decomposition.
Computational Modelling: Ab initio and DFT simulations to map Li^+ diffusion pathways and activation energies.
Eco-Friendly Processing: Green synthesis methods to replace high-temperature sintering.
Integration with Solid-State Cathodes: Optimising interface compatibility with high-voltage cathodes ($LiNi_{0.8}Mn_{0.1}Co_{0.1}O_2$).

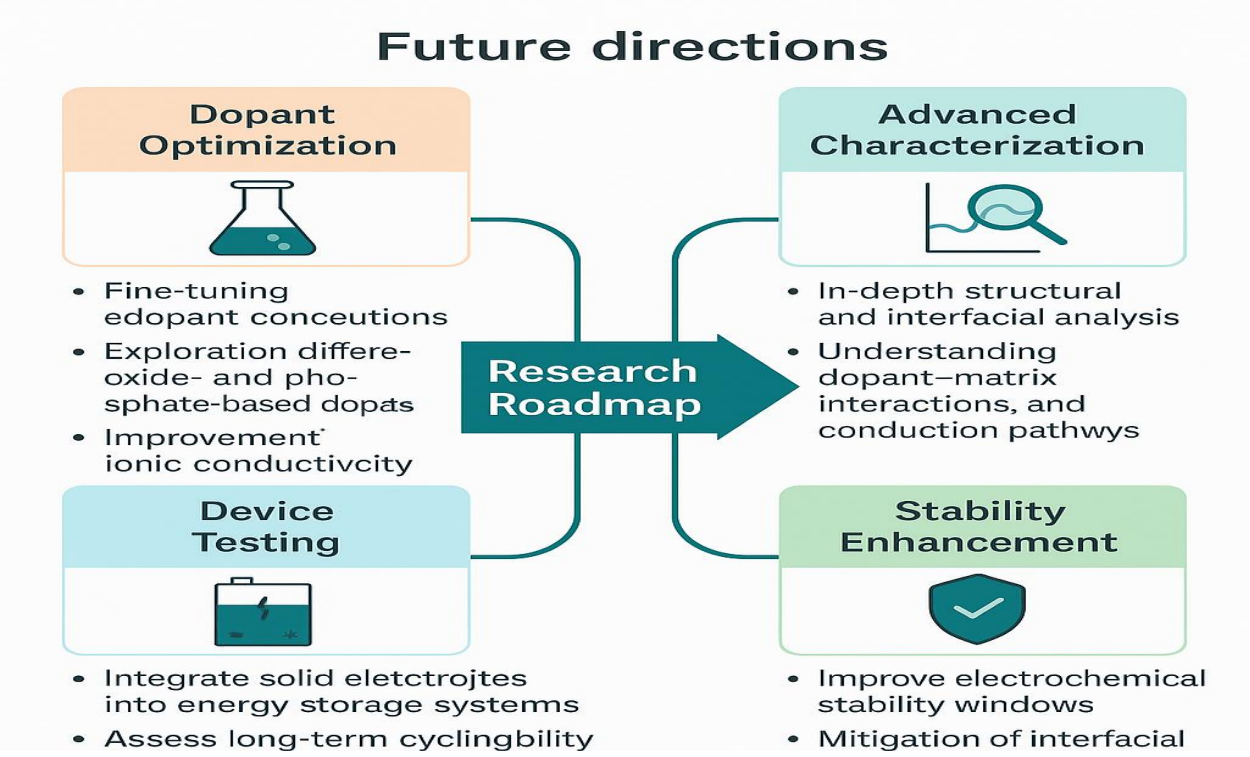

Figure 10 – Future Roadmap (Roadmap diagram showing evolution from 2024 to 2030 for Li_2SO_4-based electrolytes in SSBs.)

X. CONCLUSION

This review demonstrates that Li_2SO_4-based electrolytes, when modified with oxides such as TiO_2, ZrO_2, and B_2O_3, exhibit improved ionic conductivity (10^{-5}–10^{-4} S cm^{-1}), wider electrochemical stability (~0–4.8 V), and

International Journal of Advanced Research in Science, Engineering and Technology
ISSN: 2350-0328
Vol. 12, Issue 12, December 2025

enhanced structural integrity. Their tunable physicochemical properties make them promising candidates for next-generation all-solid-state batteries.

Further advancements in nano-doping, interface tailoring, and computational design are expected to revolutionize the applicability of Li_2SO_4 systems in sustainable, high-performance energy storage devices.

REFERENCES

1. Ganguli, M., Ghosh, A. Lithium ion transport in Li_2SO_4–Li_2O–P_2O_5 glasses. Solid State Ionics. 1999;120(1– 4):173–180.
2. Kolavekar, S.B., et al. Li ion Transport Studies in Li_2O–Li_2SO_4–ZnO–B_2O_3 glass system. AIP Conf. Proc. 2013;1536:627–628.
3. Hanumantharaju, N., et al. Li_2SO_4-doped Li_2O+B_2O_3 glasses: hopping mechanism, conductivity and dielectric relaxation. Heliyon/Materials Today: Proc. 2023.
4. Deshpande, V.K., et al. Electrical conductivity of the Li_2SO_4–Li_2CO_3 system. Electrochim. Acta. 1983;28(9):1333–1337.
5. Li, R., et al. Preparation and characterization of GDC–Li_2SO_4/Li_2CO_3 nanocomposite electrolytes for intermediate SOFCs. Ceramics International. 2017;43(17):15277–15283.
6. Hou, G., et al. A TiO_2/PEO composite incorporated with in-situ hyper-branched poly (amine-ester) as polymer electrolyte. RSC Adv. 2016;6:100089–100098.
7. Patriarchi, A., et al. All-Solid-State Li-Metal Cell Using Nanocomposite TiO_2/PEO Electrolyte. Batteries. 2023;10(1):11.
8. Moskwiak, M., et al. Ion conductivity of composite electrolyte based on PEO-DME with TiO_2 fillers. Electrochim. Acta. 2006;51(26):5904–5908.
9. Daems, K., et al. Advances in inorganic, polymer and composite electrolytes for solid-state batteries. Renew. Sustain. Energy Rev. 2024;189:113922.
10. Liang, H., et al. Tailoring practically accessible polymer/inorganic solid electrolytes. Adv. Mater. 2023;35(7):2208892.
11. Parbin, A., et al. ZrO_2 nanofiller-modified lithium phosphate solid electrolyte. J. Solid State Chem. 2024;328:123190.
12. Liu, W., et al. Improved Li-ion conductivity in composite polymer electrolytes with oxide-ion conducting nanowires. ACS Nano. 2016;10(7):7058–7066.
13. Hona, R.K., et al. Alkali ionic conductivity in inorganic glassy electrolytes: a review. J. Non-Cryst. Solids: X. 2023;18:100137.
14. Zhou, Q., et al. Increased ion conductivity in composite solid electrolytes with porous Co_3O_4 fillers. Front. Mater. 2021;8:697257.
15. Han, B., et al. Poor Stability of Li_2CO_3 in the Solid Electrolyte Interphase of Li Metal Batteries. Adv. Mater. 2021;33(30):200404.
16. Homma, K., et al. Optimizing Li_3PO_4–Li_3BO_3–Li_2SO_4 mixtures for Li-ion conductivity by machine learning. J. Phys. Chem. C. 2020;124(13):7015–7023.
17. (AIP Conf. Proc.) Electrical transport in Li_2SO_4–Li_2O–P_2O_5–B_2O_3 glassy systems with B_2O_3 addition. AIP Conf. Proc. 2025;3198:020108.
18. Jonscher, A.K. The 'universal' dielectric response. Nature. 1977;267:673–679.
19. Elliott, S.R. A.C. conduction in amorphous chalcogenide and pnictide semiconductors. Adv. Phys. 1987;36(2):135–217.
20. Patterson, A.L. The Scherrer Formula for X-Ray Particle Size Determination. Phys. Rev. 1939;56(10):978– 982.
21. Jonscher AK. The 'universal' dielectric response. Nature. 1977;267:673–679. 22.
22. Elliott SR. A.c. conduction in amorphous chalcogenide and pnictide semiconductors. Advances in Physics. 1987;36(2):135– 217.
23. Patterson AL. The Scherrer formula for X-ray particle size determination. Phys Rev. 1939;56(10):978–982. doi:10.1103/PhysRev.56.978.
24. The Arrhenius law—Activation energies and plots (teaching resource). Chem Libre Texts; 2023.
25. Randau S, Walther F, et al. Inorganic solid-state electrolytes for lithium batteries (review). Chem Rev. 2016;116(1):114–170.
26. Homma K, et al. Optimizing Li_3PO_4–Li_3BO_3–Li_2SO_4 mixtures for Li-ion conductivity by machine learning. J Phys Chem C. 2020;124(13):7015–7023.
27. Kolavekar SB, et al. Li-ion transport in Li_2O–Li_2SO_4–ZnO–B_2O_3 glass system. AIP Conf Proc. 2013;1536:627–628.
28. Gundale SS, et al. Electrical conductivity of Li_2O–B_2O_3–SiO_2–Li_2SO_4 glasses and glass-ceramics. Solid State Ionics. 2016;297:81–88.
29. Yamashita M, Terai R. Ionic conductivity of Li_2O–B_2O_3–Li_2SO_4 glasses. Glastechnische Berichte. 1990;63(1):13–17.
30. Dissanayake MAKL. Phase diagram and electrical conductivity of the Li_2SO_4–Li_2CO_3 system. Solid State Ionics. 1986;18(3–4):319–325.
31. Deshpande VK, Singh R. Electrical conductivity of the Li_2SO_4–Li_2CO_3 system. Electrochim Acta. 1983;28(9):1333–1337.
32. Nagao K, et al. Highly stable Li/Li_3BO_3–Li_2SO_4 interface and application to all-oxide batteries. ACS Appl Energy Mater. 2019;2(8):5890–5897.
33. Li J, et al. Proton conductivity and chemical stability of Li_2SO_4-based composite electrolytes. Electrochim Acta. 2006;51(26):5562–5567.
34. Dazhi W, et al. The nanometer $(Li_2SO_4)_{1-x}$–$(ZrO_2)_x$ solid composite electrolyte. Chinese J Chem Phys. 1999;12(6): (early report on ZrO_2–Li_2SO_4).
35. Materials Project. Li_2SO_4 crystal data (orthorhombic). MaterialsProject.org (accessed 2025).
36. Wu S, et al. $LiY(SO_4)_2$ superionic material; notes Li_2SO_4 transition at ~575 °C and melt at ~860 °C. arXiv :2304.08728; 2023.
37. Lunden A, et al. Electrical conductivity, self-diffusion and phase diagram of Li_2SO_4–LiBr; transition at 575 °C. Solid State Ionics. 1986;18(3–4):253–260.
38. Thermal expansion of lithium sulphate; first-order phase transition at 575 °C. (Report). Research Gate preprint.
39. Doppiu S, et al. The Li_2SO_4–Na_2SO_4 system for thermal energy storage (450–550 °C). Materials. 2019;12(22):3694.

40. Fedorov PP, et al. Phase diagram of the Li_2SO_4–Na_2SO_4 system. J Am Ceram Soc. 2020;103(4): (online early).
41. Gamry Instruments. Common equivalent circuit models (Randles cell origin—Randles 1947). White Paper; 2017.
42. Patel B, et al. Data-driven analysis of electrochemical impedance spectroscopy. Patterns. 2025;6(9):100980.
43. Elgrishi N, et al. A practical beginner's guide to cyclic voltammetry. J Chem Educ. 2018;95(2):197–206.
44. Bard AJ, Faulkner LR. Electrochemical Methods: Fundamentals and Applications, 2nd ed. Wiley; 2001.
45. Liang H, et al. Tailoring practically accessible polymer/inorganic solid electrolytes (review). Adv Mater. 2023;35(7):2208892.
46. Hou G, et al. TiO_2/PEO composite polymer electrolyte with hyper-branched modifier. RSC Adv. 2016;6:100089–100098.
47. Patriarchi A, et al. All-solid-state Li-metal cell using nanocomposite TiO_2/PEO electrolyte. Batteries. 2023;10(1):11.
48. Lee TK, et al. Polyester–ZrO_2 nanocomposite electrolytes with high Li-ion transference. Batteries & Supercaps. 2021; 4(7):
49. Zhou Q, et al. Increased ion conductivity in composite solid electrolytes with porous Co_3O_4 fillers. Frontiers in Materials. 2021;8:697257.
50. Hona RK, et al. Alkali ionic conductivity in inorganic glassy electrolytes: a review. J Non-Cryst Solids: X. 2023;18:100137.
51. Lithium sulfate—overview: superionic above ~575 °C (~0.1 S cm^{-1}). ScienceDirect Topics (accessed 2025).
52. Lunden A/Materials Project (crystal data and transition context). Supplementary crystal/DB sources.
53. (Not cited in-text) Katz E. Electrochemical contributions: John E. B. Randles (1912–1998). Electrochemistry. 2023;91(2):e202300005. (Historical context for Randles circuit).
54. Tatsumisago M, et al. Electrical & mechanical properties of Li_3BO_3–Li_2SO_4 glass and glass-ceramics; $90Li_3BO_3 \cdot 10Li_2SO_4$ conductivity. J Ceram Soc Jpn. 2017;125(6): (open-access PDF). ([J-STAGE][33])
55. Joo K-H, et al. Thin-film lithium-ion conducting LiBSO solid electrolyte (PLD). ECS Proc. 2002; 203:196.
56. Lin L, et al. Progress and perspective of glass-ceramic solid-state electrolytes (includes Li_3BO_3–Li_2SO_4 data). J Energy Chem. 2023;83: (review).

AUTHOR'S BIOGRAPHY

Full name	**Gaurav S. Chaudhari**
Science degree	M.Sc. PHYSICS
Academic rank	Research Scholar
Institution	Bapurao Deshmukh College of Engineering and Management, Sewagram, Wardha , Maharashtra, India

Full name	**Nilesh R. Thakare**
Science degree	Ph.D.
Academic rank	Independent researcher
Institution	P. R. Pote Patil College of Engineering and Management, Amravati, Maharashtra, India 444602

Full name	**Aniket Deshmukh**
Science degree	M.Sc. PHYSICS
Academic rank	Research Scholar
Institution	P. R. Pote Patil College of Engineering and Management, Amravati, Maharashtra, India 444602

International Journal of Advanced Research in Science, Engineering and Technology

Vol. 12, Issue 12, December 2025

ISSN: 2350-0328

IMPACT FACTOR 7.150

Full name	**Ajay R. Chaware**
Science degree	Ph.D.
Academic rank	Independent researcher
Institution	Bapurao Deshmukh College of Engineering and Management, Sewagram, Wardha , Maharashtra, India

Full name	**Vijeta A. Jadhav**
Science degree	M.Sc. PHYSICS
Academic rank	Research Scholar
Institution	P. R. Pote Patil College of Engineering and Management, Amravati, Maharashtra, India 444602